doi:10.3788/gzxb20144309.0906002

# 基于应力分析的电镀保护光纤布喇格光栅传感性能分析

谢剑锋[1],王颖[1],莫钊[1],刘咏松[2],曾任贤[1]

(1 南昌工程学院 信息工程学院,南昌 330099)

(2 浙江理工大学 理学院,杭州 310018)

**摘 要**:为保护光纤光栅,提出了一种镀层和光纤光栅结合良好的无粗化过程的化学镀和电镀保护方法.基于应力分析法,得到镀镍光纤光栅的温度灵敏度公式,采用 ANSYS 有限元软件分析了电镀后光纤光栅应力随温度变化关系,并进行了实验证实.结果表明:光纤光栅电镀后温度灵敏度理论和实验值分别为 20.6951 pm/℃、22.076 pm/℃.理论分析和实验、仿真结果基本一致.相比裸光纤光栅,温度灵敏度增加到原来的 2.2 倍.该方法不仅可以获得厚度理想的保护层,还可以提高光纤光栅的温度灵敏度.

**关键词**:电镀;传感性能;热应力;光纤布喇格光栅;ANSYS

**中图分类号**: **文献标识码**:A **文章编号**:1004-4213(2014)09-0906002-4

# Sensing Properties of Nickel Electroplating Protected Fiber Bragg Grating Based on Stress Analysis

XIE Jian-feng[1], WANG Ying[1], MO Zhao[1], LIU Yong-song[2], ZENG Ren-xian[1]

(1 *School of Information Engineering, Nanchang Institute of Technology, Nanchang* 330099, *China*)

(2 *College of Sciences, Zhejiang Sci-Tech University, Hangzhou* 310018, *China*)

**Abstract**: In order to protect Fiber Bragg Grating (FBG), a non-coarsening fiber surface electroless plating and electroplating technics with good adhesion force between layer and fiber was proposed. Based on stress analysis, the temperature sensitivity of protected FBG was achieved in theory, the stresses on the protected FBG under varied temperatures were analyzed by a finite element analysis software (ANSYS) and verified by experiment. The results show that the temperature sensitivity of protected FBG is 20.6951 pm/℃ theoretical and 22.076 pm/℃ from the experiments, which the results of theoretical analysis match the ones from experiments and simulations very well. The temperature sensitivity is 2.2 times as much as that of bare FBG. The desirable thickness of metallic protect layer can be obtained and the temperature sensitivity can be improved.

**Key words**: Electroplating; Sensing properties; Thermal stress; FBG; ANSYS

**OCIS Codes**: 060.2300; 060.2370; 060.2400; 160.3900; 240.0310

## 0 Introduction

The utilization of optical fiber gauges to measure temperature, strain, or even to detect fracture in a material has great potential due to their relatively small size, sensitivity, and insensitivity to electrical fields[1-7].

Embedding the optical fibers is challenging when they need to be embedded in a metal structure, which has a high melting temperature[8]. Obviously, the optical fiber needs protection during the high-temperature deposition steps. In particular, a protective layer may be necessary to solve the temperature and stress problems caused by the embedding process.

**Foundation item**: The National Natural Science Foundation of China (No. 21274132), the Scientific Research Foundation of Jiangxi Provincial Education Department( No. GJJ08451).

**First author**: XIE Jian-feng(1971—), male, Associate Professor, Ph. D. degree, mainly focuses on fiber smart structure and fiber grating sensing technology. Email: uestcxjf@163.com

**Received**: Dec. 4, 2013; **Accepted**: Mar. 6, 2014

*http://www.photon.ac.cn*

Since an optical fiber is basically made of $SiO_2$, an electrically conductive coating is needed to serve as a “seed” for electroplating. This conductive layershould be thin and capable of bonding well with the optical fiber. We selected electroless plating to deposit the metallic thin film[9].

In this paper, a non-coarsening fiber surface electroless plating technics with good adhesion force between layer and fiber was proposed. Electroplating and electroless plating are applied in the Fiber Bragg Grating(FBG) protected process. The stresses on FBG in axial and cross directions were analyzed. The temperature sensitivity of nickel clad FBG is achieved in theory based on stress analysis. A finite element analysis software(ANSYS) was used to simulate the stresses on the protected FBG.

## 1 Theoretical analysis

The schematic diagram of protected FBG is shown in Fig. 1. where, ( $x$ , $y$ , $z$ ) are Cartesian coordinate

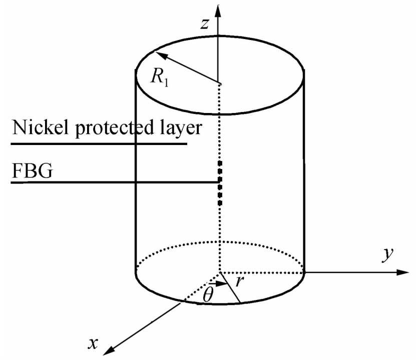


Fig. 1 Schematic diagram of nickelprotected FBG

system, ( $r$, $\theta$, $z$ ) are Polar coordinate system. The stresses $\sigma_{r_0}$, $\sigma_{\theta_0}$ and $\sigma_{z_0}$ of protected FBG can be determined from the following equations[6-7]

$$\begin{bmatrix}\sigma_{r_i}\\ \sigma_{\theta_i}\\ \sigma_{z_i}\end{bmatrix}=\begin{bmatrix}\lambda_i+2\mu_i & \lambda_i & \lambda_i\\ \lambda_i & \lambda_i+2\mu_i & \lambda_i\\ \lambda_i & \lambda_i & \lambda_i+2\mu_i\end{bmatrix}\begin{bmatrix}\varepsilon_{r_i}-\alpha_i\Delta T\\ \varepsilon_{\theta_i}-\alpha_i\Delta T\\ \varepsilon_{z_i}-\alpha_i\Delta T\end{bmatrix} \quad (1)$$

where $\lambda_i=\dfrac{v_iE_i}{(1+v_i)(1-2v_i)}$, $\mu_i=\dfrac{v_i}{2(1+v_i)}$ , $i$ is the layer index, the FBG is referred to as layer 0. Assuming the parameters of nickel electroless plating layer and nickel electroplating layer are same, the nickel protected layer is referred to as layer 1. $\sigma_{r_i}$、$\sigma_{\theta_i}$、$\sigma_{z_i}$ represent the thermal stresses in layer $i$ ; $\varepsilon_{r_i}$、$\varepsilon_{\theta_i}$、$\varepsilon_{z_i}$ represent the total mechanical and thermal strains in layer $i$ ; $\alpha_i$ is the thermal expansion coefficient of layer $i$ ; $E_i$ is the Young′s modulus of layer $i$ ; $\nu_i$ is the Poisson ratio of layer $i$. Assuming a uniform temperature distribution in the protected FBG, the strains can be solved from the lamé solutions and expressed as the following[10-11].

$$\varepsilon_{r_i}=U_{0_i}+\frac{U_{1_i}}{r^2},\ \varepsilon_{\theta_i}=U_{0_i}-\frac{U_{1_i}}{r^2},\ \varepsilon_{z_i}=W_{0_i} \quad (2)$$

where $U_{0_i}$, $U_{1_i}$, $W_{0_i}$ are lamé constants. They can be determined from the following boundary conditions[11]

$$\sigma_{r_0}\big|_{r=R_0}=\sigma_{r_1}\big|_{r=R_0} \quad (3)$$

$$u_{r_0}\big|_{r=R_0}=u_{r_1}\big|_{r=R_0} \quad (4)$$

$$\sigma_{r_1}\big|_{r=R_1}=0 \quad (5)$$

$$\sum_{z=0}^{1}\sigma_{z_i}S_i=0 \quad (6)$$

$$\varepsilon_{z_0}=\varepsilon_{z_1} \quad (7)$$

$$U_{1_0}=0 \quad (8)$$

where $S_i$ represents the cross section of layer $i$ and the displacement $u_{r_i}$ is defined as $u_{r_i}=\int\varepsilon_{r_i}\,dr$. Eq. 3 and 4 state that the radial stresses and the displacements are continuous across the interface between the FBG and nickel-clad layer, and Equations 5 and 6 show that no external force is applied; Eq. 7 states that the end effect is ignored, and Eq. 8 states that it is impossible that the strains $\varepsilon_{r_0}$、$\varepsilon_{\theta_0}$ are infinity.

The radius of bare FBG is 62.5 $\mu$m, the radius of protected FBG is far larger than that of bare FBG. We can consider that

$$R_1\gg R_0,\ S_1\gg S_0 \quad (9)$$

From Eq. 1 to 9, we can obtain

$$\begin{cases}\sigma_{r_0}=\sigma_{\theta_0}=\dfrac{(\alpha_1-\alpha_0)E_0\Delta T}{1+\dfrac{(1+\nu_1)E_0}{(1+\nu_0)E_1}-2\nu_0}\\[2ex] \sigma_{z_0}=\dfrac{\left[1+\dfrac{(1+\nu_1)E_0}{(1+\nu_0)E_1}\right](\alpha_1-\alpha_0)E_0\Delta T}{1+\dfrac{(1+\nu_1)E_0}{(1+\nu_0)E_1}-2\nu_1}\end{cases} \quad (10)$$

where $\sigma_{r_0}$、$\sigma_{z_0}$ represent the thermal stresses of FBG. Eq. 5 shows that the thermal stresses of FBG has a good linear relation with the temperature change($\Delta T$).

There is a big difference between the bare and the protected FBG in temperature sensitivity, due to the mismatch of the thermal expansion coefficients of the fiber with those of the electroplated layer. Nickel protected layer would generate stresses on FBG in axial and cross directions when temperature is changed. The generated stresses would lead to wavelength shift and influence the temperature sensitivity of FBG. Wavelength shifts are caused by the free expansion $\Delta\lambda_{B_1}$、stresses of axial $\Delta\lambda_{B_2}$ and cross directions $\Delta\lambda_{B_3}$. The total wavelength shifts of protected FBG are the addition of $\Delta\lambda_{B_1}$, $\Delta\lambda_{B_2}$ and $\Delta\lambda_{B_3}$. That is

$$\Delta\lambda_{B_z}=\Delta\lambda_{B_1}+\Delta\lambda_{B_2}+\Delta\lambda_{B_3} \quad (11)$$

where

$$\Delta\lambda_{B_1}=\lambda_B\alpha_n\Delta T+\lambda_B\left\{\alpha_0-\frac{n_{\mathrm{eff}}^2}{2}\left[(p_{11}+2p_{12})\alpha_0\right]\right\}\Delta T \quad (12)$$

$$\Delta\lambda_{B_2}=\frac{\sigma_{z_0}\lambda_B}{E_0}\left\{1-\frac{n_{\mathrm{eff}}^2}{2}\left[p_{12}-(p_{11}+p_{12})\nu_0\right]\right\} \quad (13)$$

$$\Delta\lambda_{B_3}=\frac{-\sigma_{r_0}\lambda_B}{E_0}\left\{2v_0-\frac{n_{\mathrm{eff}}^2}{2}\left[2\nu_0p_{12}-(p_{11}+p_{12})\cdot\right.\right.$$

$$(1-\nu_0)\Big]\Big\}\tag{14}$$

The temperature sensitivity of protected FBG is

$$\Delta\lambda_{BZ}/\Delta T=(\Delta\lambda_{B_1}+\Delta\lambda_{B_2}+\Delta\lambda_{B_3})/\Delta T\tag{15}$$

where, $\alpha_n=\frac{1}{n_{eff}}\frac{\partial n_{eff}}{\partial T}$ is the thermo-optical coefficient of the FBG, $\lambda_B$ is reflected wavelength of FBG, $p_{11}$、$p_{12}$ are the Pockels coefficients of the FBG, $n_{eff}$ is the refractive index of the FBG.

Parameters of FBG (provided by Shanghai SynetOptics Technology Co.) are: $\nu_0=0.17$, $\alpha_0=0.55\times10^{-6}/℃$, $E_0=7.4\times10^{10}$ Pa, $\alpha_n=6.3\times10^{-6}/℃$, $\lambda_B=1\,542$ nm, $p_{11}=0.121$, $p_{12}=0.27$, $n_{eff}=1.468\,2$, $R_0=62.5$ μm, parameters of nickel protected layer (Ni-P alloy) are: $\alpha_1=1.42\times10^{-5}/℃$[12], $\nu_1=0.31$, $E_1=1.96\times10^{11}$ Pa[12]. From Eq. 10 to 15, we could obtain that the temperature sensitivity of protected FBG is 20.695 1 pm/℃ in theory.

# 2 Experiments

## 2.1 Protection techniques of FBG

To obtain a complete and perfect nickel film, surface treatment for the FBG is necessary before electroless plating. At first, the FBGs are sensitized in a solution containing tin chloride ($SnCl_2\cdot 2H_2O$) and hydrochloric acid (HCl) in a 5 g－5 ml/100 ml for 10－12 min. Then FBGs are activated in a solution containing palladium chloride ($PdCl_2$) and hydrochloric acid in a 0.1 g－1 ml/100 ml solution for 10－12 min. Following the activated FBG process, the FBGs are then placed into an electroless nickel plating solution. The optimum conditions are: $NiSO_4\cdot 6H_2O$: 25 g/L, $NaH_2PO_2\cdot H_2O$: 20 g/L, $C_3H_6O_2$: 20 ml/L, $H_3BO_3$: 20 g/L, NaF: 1 g/L, saccharin: 2 mg /L, pH: 4.5, temperature: 86 ℃. Fig. 2 shows the experiment equipment and results of electroless plating[13].

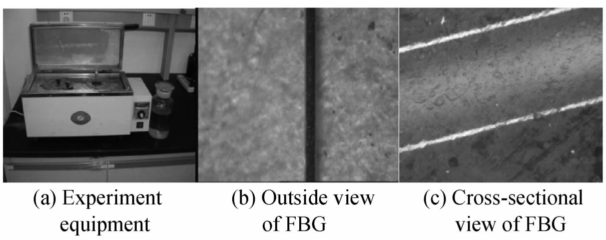


Fig. 2 Experiment equipment and results of electroless plating

After electroless nickel plating, the FBGs are placed into an nickel electroplating solution. The optimum conditions are: $NiSO_4.6H_2O$: 300 g/L, NiCl: 40 g/L, $H_3BO_3$: 40 g/L, $C_{12}H_{25}SO_4Na$: 0.1-0.3 g/L, saccharin: 1-3g/L, ph: 3.9-4.2, temperature: 50-60℃, current density: 0.03-0.04 A/cm$^2$. The experiment equipment and results of electroplating are show in Fig. 3. Fig. 3(c) shows that the diameter of protected FBG is 1 761.37 μm and the diameter of bare FBG is 125 μm.

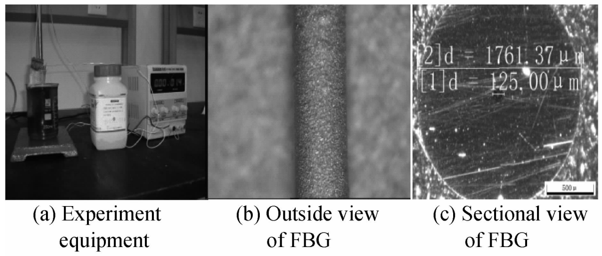


Fig. 3 Experiment equipment and results of electroplating

## 2.2 Sensing characteristic of protected FBG

The protected FBG was placed in a temperature-controlled oven to study the temperature sensitivity. The shift of the Bragg wavelength corresponding to the varied temperature was monitored with a FBG Network Analyzer (Shanghai SynetOptics Technology Co.). The protected FBG was subjected to different testing temperatures from 60 to 200℃ at 20℃ interval. At each testing temperature, a specimen is held for approximately 30 min to achieve thermal equilibrium. The wavelength shifts was recorded every minute using a FBG Network Analyzer for approximately 15-20 min and averaged.

Experiment results in Fig. 4 shows that the wavelength shift of protected FBG sensors are proportional to the temperature change, and the temperature sensitivity is 22.076 pm/℃. There is a big difference between the bare and the protected FBG in temperature sensitivity, due to the mismatch of the thermal expansion coefficients of the fiber with those of the electroplated layer. The temperature sensitivity is 2.2 times as much as that of bare FBG.

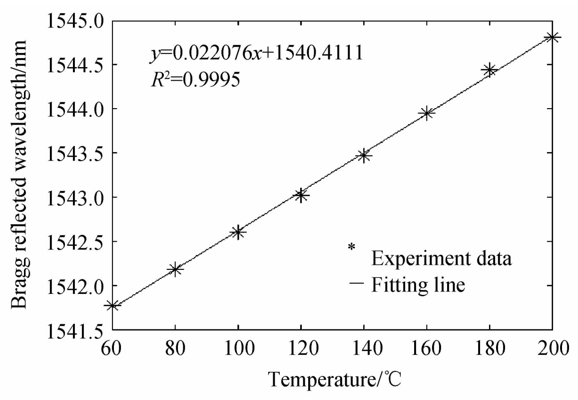


Fig. 4 Experiment results of temperature sensitivity (protected FBG)

# 3 Finite element analysis

The stresses and strains on the protected FBG and protected layer under varied temperature were numerically analyzed by using a finite element method. Assuming that the FBG and nickel protected layer are well-knit and the temperature difference is 10℃, we must "glue" the FBG to the nickel protected layer and temperature is changed from 20℃ to 30℃ (reference temperature is 20℃). The stresses of finite element analysis are show in Fig. 5 and Fig. 6.

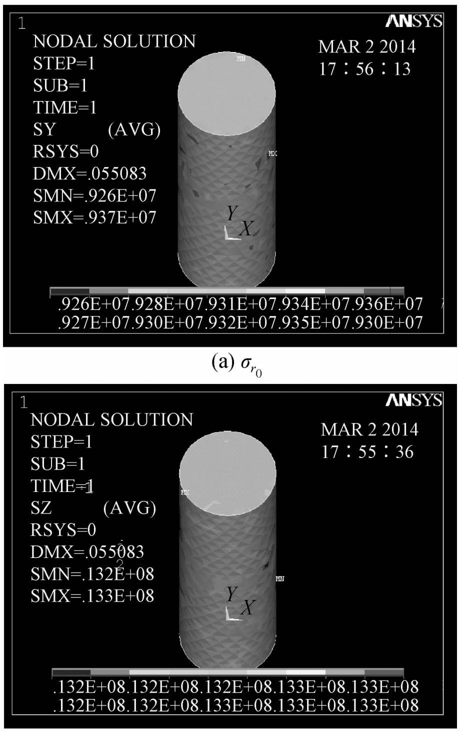


(a) $\sigma_{r_0}$

(b) $\sigma_{Z_0}$

Fig. 5 Simulation results of stresses on FBG

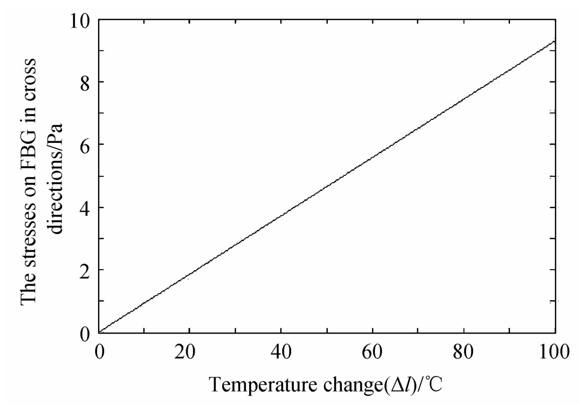


Fig. 6 The relationship between $\sigma_{r_0}$ and $\Delta T$

Fig. 5 shows that $\sigma_{r_0} \approx 9.3\times10^6$, $\sigma_{z_0} \approx 1.32\times10^7$ in simulation. According to Eq. 10, we can obtain, $\sigma_{r_0} = 9.3054\times10^5\Delta T$ pa, $\sigma_{z_0} = 1.3251\times10^6\Delta T$ pa in theory. Eq. 10 shows that the thermal stresses of FBG has a good linear relation with the temperature change ($\Delta T$). Fig. 6 shows the relationship between $\sigma_{r_0}$ and $\Delta T$. The results of theoretical analysis match the simulation very well.

# 4 Conclusions

After FBG was protected by nickel clad layer, nickel clad layer would generate stresses on FBG in axial and cross directions when temperature is changed. This is due to the different thermal expansion coefficient between FBG and protected layer. The generated stresses would lead to wavelength shift and influence the temperature sensitivity of FBG. The stresses on FBG in axial and cross directions were analyzed. The temperature sensitivity of protected FBG is 20.695 1 pm/℃ in theory and 22.076 pm/℃ from experiment. In this paper the FBG was protected well and the temperature sensitivity is 2.2 times as much as that of bare FBG. The analysis of the experiment shows that the desirable thickness of metallic protect layer can be obtained and the temperature sensitivity can be improved.

References

[1] ZHAN Ya-ge, CAI Hai-wen, GENG Jian-xin, *et al*. Study on aluminum groove encapsulating technique and sensing characteristics of FBG sensor[J]. *Acta Photonica Sinica*, 2004, **33**(8): 952-955.

[2] SHU Yue-jie, CHEN Wei-min, ZHANG Peng, *et al*. Investigation on evaluation theory of fiber bragg grating tensile fatigue property[J]. *Acta Photonica Sinica*, 2013, **42**(7): 805-811.

[3] WU Ru-jun, ZHENG Bai-lin, HE Peng-fei, *et al*. Influence of encapsulation structures for embedded fiber-optic Bragg grating sensors on strain measurement[J]. *Optics and Precision Engineering*, 2014, **22**(1): 24-30.

[4] ZHANG Jing-hua, QIAO Xue-guang, FENG Zhong-yao, *et al*. Fiber-optical grating sensing based on flextensional member[J]. *Acta Physica Sinica*, 2012, **61**(5): 054215.

[5] LI Zhi, YANG Ming-hong, DAI Ji-xiang, *et al*. Improvment research of fiber-optic hydrogen gas sensor using pt catalyzed tungsten trioxide[J]. *Acta Photonica Sinica*, 2013, **42**(9): 1046-1051.

[6] CAO Ye, PEI Yong-wei, TONG Zheng-rong. Simultaneous measurement of temperature and bending-curvature using a single local micro-structured longperiod fiber grating[J]. *Acta Physica Sinica*, 2014, **63**(2): 024206.

[7] SUN Li, SUN Qian-qian, REN Liang, *et al*. A new method for underground pipeline corrosion monitoring applied FBG[J]. *Acta Photonica Sinica*, 2012, **41**(1): 6-10.

[8] LI Xiao-chun. Embedded sensors in layered manufacturing[D]. Dissertation Abstracts International, 2001, 62(10), Section: B,4745. Adviser: Fritz Prinz, Stanford University.

[9] RAO Chun-fang, ZHANG hua, FENG Yan, *et al*. Heat treatment on fiber Bragg grating with Ni coating for elevbated temperature sensor[J]. *Optics and Precision Engineering*, 2011, **19**(9): 2006-2013.

[10] CHENG Chang-jun. Elastic mechanics[M]. Lanzhou: Lanzhou University Press, 1996, 467.

[11] SHYU C T, WANG L. Sensitive linear electric current measurement using two metal-coated single-mode optical fibers[J]. *Journal of Lightwave Technology*, 1994, **12**(11): 2040-2048.

[12] HE Jian-bo, WU Xiao-an, HUAN Hui, *et al*. A review of study of electroplating of amorphous Ni-P alloy and prospects of its applications[J]. *Journal of Zhejiang University of Technology*, 1999, **27**(1): 62-70.

[13] SONG Lu-fa, ZHANG Hua, XIE Jian-feng, *et al*. Experimental study on temperature sensing property for electroless Ni-plating fiber Bragg grating[J]. *Acta Photonica Sinica*, 2007, **36**(11): 2022-2024.